Interaction of Acetylene and Cyanide with the Resting State of Nitrogenase α-96-Substituted MoFe Proteins†

Paul M. C. Benton,‡ Suzanne M. Mayer,§ Junlong Shao,|| Brian M. Hoffman,|| Dennis R. Dean,*,§ and Lance C. Seefeldt*,‡

Department of Chemistry and Biochemistry, Utah State University, Logan, Utah 84322, Department of Biochemistry, Virginia Tech, Blacksburg, Virginia 24061, and Department of Chemistry, Northwestern University, Evanston, Illinois 60208

Received July 27, 2001; Revised Manuscript Received September 26, 2001

ABSTRACT: The nitrogenase MoFe protein contains the active site metallocluster called FeMo-cofactor [7Fe-9S-Mo-homocitrate] that exhibits an $S = 3/2$ EPR signal in the resting state. No interaction with FeMo-cofactor is detected when either substrates or inhibitors are incubated with MoFe protein in the resting state. Rather, the detection of such interactions requires the incubation of the MoFe protein together with its obligate electron donor, called the Fe protein, and MgATP under turnover conditions. This indicates that a more reduced state of the MoFe protein is required to accommodate substrate or inhibitor interaction. In the present work, substitution of an arginine residue (α-96^{Arg}) located next to the active site FeMo-cofactor in the MoFe protein by leucine, glutamine, alanine, or histidine is found to result in MoFe proteins that can interact with acetylene or cyanide in the as-isolated, resting state without the need for the Fe protein, or MgATP. The dithionite-reduced, resting states of the α-96^{Leu}-, α-96^{Gln}-, α-96^{Ala}-, or α-96^{His}-substituted MoFe proteins show an $S = 3/2$ EPR signal ($g = 4.26, 3.67, 2.00$) similar to that assigned to FeMo-cofactor in the wild-type MoFe protein. However, in contrast to the wild-type MoFe protein, the α-96-substituted MoFe proteins all exhibit changes in their EPR spectra upon incubation with acetylene or cyanide. The α-96^{Leu}-substituted MoFe protein was representative of the other α-96-substituted MoFe proteins examined. The incubation of acetylene with the α-96^{Leu} MoFe protein decreased the intensity of the normal FeMo-cofactor signal with the appearance of a new EPR signal having inflections at $g = 4.50$ and 3.50. Incubation of cyanide with the α-96^{Leu} MoFe protein also decreased the FeMo-cofactor EPR signal with concomitant appearance of a new EPR signal having an inflection at $g = 4.06$. The acetylene- and cyanide-dependent EPR signals observed for the α-96^{Leu}-substituted MoFe protein were found to follow Curie law $1/T$ dependence, consistent with a ground-state transition as observed for FeMo-cofactor. The microwave power dependence of the EPR signal intensity is shifted to higher power for the acetylene- and cyanide-dependent signals, consistent with a change in the relaxation properties of the spin system of FeMo-cofactor. Finally, the α-96^{Leu}-substituted MoFe protein incubated with ^{13}C-labeled cyanide displays a ^{13}C ENDOR signal with an isotropic hyperfine coupling of 0.42 MHz in Q-band Mims pulsed ENDOR spectra. This indicates the existence of some spin density on the cyanide, and thus suggests that the new component of the cyanide-dependent EPR signals arise from the direct bonding of cyanide to the FeMo-cofactor. These data indicate that both acetylene and cyanide are able to interact with FeMo-cofactor contained within the α-96-substituted MoFe proteins in the resting state. These results support a model where effective interaction of substrates or inhibitors with FeMo-cofactor occurs as a consequence of both increased reactivity and accessibility of FeMo-cofactor under turnover conditions. We suggest that, for the wild-type MoFe protein, the α-96^{Arg} side chain acts as a gatekeeper, moving during turnover in order to permit accessibility of acetylene or cyanide to a specific [4Fe-4S] face of FeMo-cofactor.

The reduction of dinitrogen to ammonia during biological nitrogen fixation is catalyzed by the metalloenzyme nitrogenase [for recent reviews, see (*1*−*3*)]. The Mo-dependent nitrogenase is composed of an Fe protein[1] component, which possesses a single [4Fe-4S] cluster (*4*) and is the obligate electron donor to the MoFe protein component (*5*). The $\alpha_2\beta_2$ MoFe protein contains two active site FeMo-cofactors [7Fe-9S-Mo-homocitrate] and two electron-transfer intermediate P-clusters [8Fe-7S] (*6*), with one of each metal cluster type contained in an individual $\alpha\beta$-catalytic unit (*7, 8*). During catalysis, the Fe protein delivers one electron at a time (*9*) to an $\alpha\beta$ unit of the MoFe protein in a process coupled to the hydrolysis of two MgATP molecules. Each electron is

† This work was supported by National Institutes of Health Grant R01-GM59087 (to L.C.S. and D.R.D.) and National Science Foundation Grant MCB-9904018 (to B.M.H.).

* Address correspondence to these authors. L.C.S.: phone (435) 797-3964, fax (435) 797-3390, email seefeldt@cc.usu.edu. D.R.D.: phone (540) 231-5895, fax (540) 231-7126, email deandr@vt.edu.

‡ Utah State University.

§ Virginia Tech.

|| Northwestern University.

[1] Abbreviations: Fe protein, iron protein; MoFe protein, molybdenum−iron protein; FeMo-cofactor, iron−molybdenum cofactor; EPR, electron paramagnetic resonance; ENDOR, electron−nuclear double resonance.

10.1021/bi011571m CCC: $20.00 © 2001 American Chemical Society
Published on Web 10/26/2001

initially delivered to a P-cluster and ultimately to the FeMo-cofactor where substrates are bound and reduced (*10*). Following each electron-transfer event, the Fe protein is believed to dissociate from the MoFe protein, completing one intercomponent electron-transfer cycle (*11*). This cycle is sequentially repeated, resulting in progressively more reduced states of the MoFe protein (designated as E_0, E_1, E_2, etc.) until sufficient electrons have accumulated to permit substrate binding and reduction to occur (*12*). In addition to dinitrogen, nitrogenase also reduces protons and a range of doubly and triply bonded compounds (e.g., acetylene) by multiples of two electrons (*13*). A detailed description of the site and nature of substrate or inhibitor binding to FeMo-cofactor remains an important but unknown aspect about the nitrogenase mechanism. The solution of X-ray structures for MoFe proteins from *Azotobacter vinelandii* (*8, 14, 15*), *Clostridium pasteurianum* (*16*), and *Klebsiella pneumoniae* (*17*) has revealed the FeMo-cofactor structure, which in turn has led to different models for how substrates might bind (*15, 18*−*27*). A difficulty with characterizing MoFe protein with substrate or inhibitor bound to FeMo-cofactor is that binding is only detected under turnover conditions when MoFe protein, Fe protein, MgATP, and a source of reducing equivalents are present (*28, 29*). Spectroscopic characterization of nitrogenase quenched during turnover in the presence of the inhibitor CO (*30*−*35*), or the substrates nitrogen (*31*), protons (*30, 36, 37*), acetylene (*37*−*39*), and CS_2 (*40*), or the product ethylene (*41*) has provided some information about intermediate states and possible binding sites to FeMo-cofactor. Likewise, pre-steady-state and steady-state kinetic studies with nitrogenases during turnover have provided insights into the nature of the mutual interactions among various substrates and inhibitors with the active site (*2*). Collectively, these observations indicate that accumulation of electrons within the MoFe protein during turnover results in changes in the reactivity of FeMo-cofactor toward substrates or inhibitors, or that changes in the FeMo-cofactor polypeptide environment occur during turnover in order to permit substrate or inhibitor access. These possibilities are not mutually exclusive.

We previously reported that substitution of the α-69^{Gly} residue by Ser within the MoFe protein from *Azotobacter vinelandii* affected the reduction of acetylene but not dinitrogen (*42, 43*). This finding was interpreted to indicate that the [4Fe-4S] face of FeMo-cofactor capped by the adjacent residue, α-70^{Val}, possibly serves as an acetylene reduction site (lighter colored Fe and S atoms in Figure 1, panels A and B). In support of this model, it has been found that substitution of the α-70^{Val} residue by Ala results in an altered MoFe protein that can effectively reduce short-chain alkynes, such as propargyl alcohol and propyne, which otherwise are only very poor substrates for the wild-type MoFe protein (*44*). Likewise, certain amino acid substitutions at the α-195^{His} residue position, which is located near the same [4Fe-4S] face, also have some affect on substrate and inhibitor interactions with FeMo-cofactor (*45*−*52*). Inspection of the MoFe protein resting state structure shows that residues surrounding the FeMo-cofactor are so tightly packed there does not appear to be sufficient room to accommodate substrate or inhibitor interaction at this [4Fe-4S] face. Thus, a model where this [4Fe-4S] face of FeMo-cofactor provides a substrate interaction site demands the movement of either or both α-70^{Val} and α-96^{Arg} to accommodate interaction with substrates. To test whether such movement of the α-96^{Arg} side chain might be involved in providing substrate or inhibitor access to FeMo-cofactor, we asked if altered MoFe proteins having substitutions at the α-96^{Arg} position are able to interact with substrates or inhibitors in the resting state.

EXPERIMENTAL PROCEDURES

Protein Isolation and Activity Assays. Wild-type Fe protein and polyhistidine-tagged MoFe proteins were expressed in *A. vinelandii* cells (*53*) and purified to homogeneity as previously described (*54*). The specific activity for C_2H_2 reduction catalyzed by wild-type nitrogenase was ~2000 nmol of product min^{-1} (mg of protein)$^{-1}$. Amino acid substituted MoFe proteins were isolated from *A. vinelandii* strains designated DJ1264 (α-96^{Gln}), DJ1328 (α-96^{Leu}), DJ1336 (α-96^{His}), and DJ1327 (α-96^{Ala}). Methods for strain construction, large-scale cell growth, protein purification, and handling were done as reported previously (*42, 55, 56*). All protein manipulations were conducted in the absence of oxygen in septum-sealed serum vials under an argon atmosphere. All anaerobic liquid and gas transfers were performed using gastight syringes. Acetylene reduction assays were performed as previously described (*56*).

Preparation of MoFe Proteins with Substrates or Inhibitors. MoFe protein samples (20 mg/mL unless stated otherwise) with acetylene, CO, N_2, or propyne were prepared in 100 mM MOPS buffer, pH 7.0, with 2 mM sodium dithionite ($Na_2S_2O_4$) under argon with various partial pressures of the appropriate gas. Samples were allowed to incubate for 3 min at 25 °C after which time a 250 μL aliquot was transferred into septum-sealed 4 mm quartz EPR tubes and immediately frozen in liquid nitrogen. MoFe protein samples (20 mg/mL) with cyanide or azide were prepared in 50 mM Tris buffer, pH 8.0, with 2 mM sodium dithionite under argon. Samples for the analysis of the effect of pH on the cyanide-induced signals were prepared in a combination 50 mM Tris and 50 mM MES buffer at pH values of 6.5, 7.5, or 8.5 with 2 mM sodium dithionite and under argon. Sodium cyanide was added to the indicated concentration from a 0.1 M stock solution. Proteins were allowed to incubate for 3 min at 25 °C and then frozen in EPR tubes. Given the equilibrium between HCN and CN^- with a pK_a of 9.11 (*57*), both species are present at the pH values examined. Hence, we refer to cyanide to indicate the sum of the concentrations of HCN and CN^-. The reversibility of the acetylene- or cyanide-dependent EPR changes was evaluated by passage of the appropriately treated MoFe protein sample through a Sephadex G-25 column equilibrated with 50 mM Tris buffer, pH 8.0, with 300 mM NaCl and 2 mM dithionite. The protein was transferred immediately to a septum-sealed EPR tube and frozen in liquid nitrogen.

The effect of pH on the resting state EPR spectrum of the α-96^{Leu} MoFe protein was also investigated for samples prepared in the above combination buffer at pH values of 6.5, 7.5, or 8.5 with 2 mM sodium dithionite and under argon.

EPR Spectroscopy. X-band EPR spectroscopy was performed using a Bruker ESP-300E spectrometer equipped with an ER 4116 DM dual-mode X-band cavity and an Oxford Instruments ESR-900 helium flow cryostat. In all cases, calibrated 4 mm quartz EPR tubes (Wilmad, Buena, NJ) were

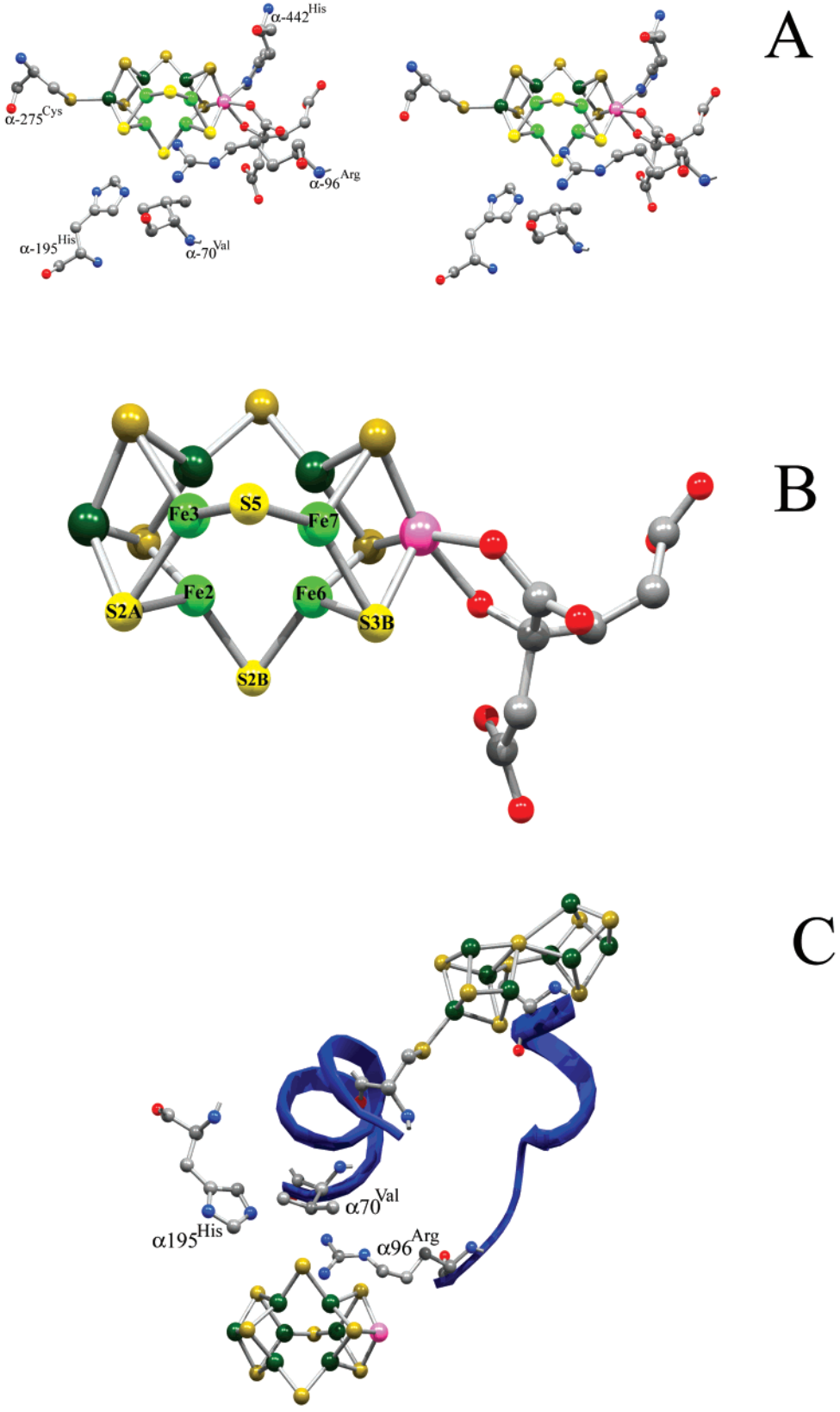

FIGURE 1: FeMo-cofactor protein environment. (Panel A) Stereoview of FeMo-cofactor (including homocitrate on the right) and the ligands α-275^{Cys} and α-442^{His}. The positions of α-96^{Arg}, α-70^{Val}, and α-195^{His} are also shown. The four Fe atoms on the side of FeMo-cofactor facing α-96^{Arg} are shown in lighter green and the four S atoms in lighter yellow. (Panel B) FeMo-cofactor with the four S and four Fe atoms on the side facing α-96^{Arg} shown in lighter colors and labeled as Fe2, Fe3, Fe6, and Fe7 and S2A, S2B, S3B, and S5 as previously designated (*8*). (Panel C) The P-cluster (top right), the αC trace of peptides (blue ribbons) between the P-cluster and α-70^{Val} and α-96^{Arg}, and FeMo-cofactor (without homocitrate) are shown. The figures were generated from the MoFe protein coordinates (*8*) using the Swiss-PDB Viewer program (*78*). Atom colors are carbon in gray, nitrogen in blue, molybdenum in pink, sulfur in yellow, and iron in green.

used. Independently recorded background spectra of the cavity were aligned with and subtracted from experimental spectra. EPR spectra were recorded at a modulation frequency of 100 kHz and a modulation amplitude of 1.26 mT (12.6 G) with a sweep rate of 10 mT s^{-1}. Spectra were recorded at microwave frequencies of approximately 9.64 GHz, with the precise microwave frequencies recorded for individual spectra to ensure exact g-alignment. Operating temperature and other EPR parameters are specified in the figure legends for individual samples. Subsequent manipulations of spectral data (including the generation of all graphical representations) were accomplished using the program Igor Pro (WaveMetrics, Lake Oswego, OR). Simulations were done using software written by Dr. Mike Hendrich (Carnegie Mellon University) and combine singled-valued decomposition with least-squares fitting to match a sum of simulations to the spectrum. Relative amounts of each species were determined for an $S = 3/2$ system where intrinsic g values, $g_x = g_y \neq g_z$ (both approximately equal to 2.00), and E/D were allowed to vary independently. Integration of the EPR signals was relative to the integrated area for the $S = 3/2$ signal of the resting wild-type MoFe protein.

Q-band EPR spectra were recorded on a modified Varian E-110 ENDOR capable cw spectrometer, at 2 K in dispersion mode, using 100 kHz field modulation under "rapid passage" conditions. The spectra represent the absorption line shape, not its derivative (*58*, *59*).

Temperature and Power Dependence of EPR Signals. The nonsaturating microwave power at 5 K was established for all EPR signals using plots of EPR signal intensity versus the square root of the microwave power. The optimum nonsaturating microwave powers for acetylene- and cyanide-treated samples were 0.32 and 2.01 mW, respectively. X-band EPR spectra were recorded for each sample at the optimal nonsaturating microwave power at different temperatures. The relative peak height for each EPR signal was plotted against the temperature, and the data were fit to the Curie law $1/T$ dependence described by eq 1:

$$S = k/T + x \quad (1)$$

where S is the EPR signal intensity, k is an arbitrary constant, T is the temperature in degrees kelvin, and x is a correction factor. For the cyanide- and acetylene-treated MoFe protein samples, k varied from 5.0 to 6.9 and x from -0.06 to -0.52. Curie law strictly holds for isolated spin systems, usually $S = 1/2$. When $S > 1/2$, low-lying excited states become populated with increasing temperatures, which decreases the population of the lowest spin level at a greater rate than that predicted by Curie law. However, in the present case, the excellent agreement of the data with Curie law and the complete absence of new signals in the EPR spectra at higher temperatures due to non-Curie-law-dependent transitions constitute evidence not only that the signals are due to ground-state transitions but also that there are no low-lying excited states within the temperature range examined in these experiments. For the microwave power dependence of the EPR signals, spectra (the sum of 10 scans) were acquired at 5 K and at microwave powers from 0.1 to 20.1 mW. The microwave power was taken as that recorded from the bridge. The actual power at the sample may be different from that reported, and thus will depend on the spectrometer. The relative intensity of the EPR signals was adjusted to a common value for the purposes of the graph shown in Figure 8. Data were fit to a single exponential. Such fits have no theoretical significance, but rather are used to track the data.

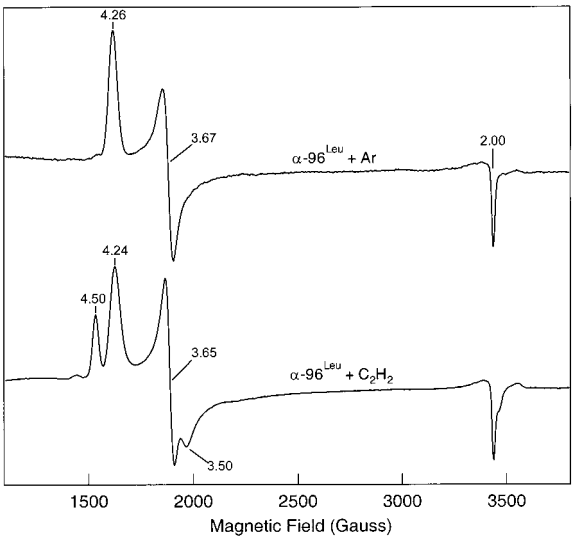

FIGURE 2: EPR spectra of α-96^{Leu} MoFe protein under nonturnover conditions with acetylene. The α-96^{Leu} MoFe protein was prepared under a gas phase of either 1.0 atm of argon (top trace) or 1.0 atm of acetylene (bottom trace). The X-band EPR spectra were recorded at a temperature of 5 K, and a microwave power of 2.0 mW. Each trace represents the sum of 5 scans.

ENDOR Spectroscopy. MoFe protein samples (100 mg/mL) with [^{13}C]cyanide for ENDOR analysis were prepared in 50 mM Tris buffer, pH 8.0, using ^{13}C-labeled NaCN (Cambridge Isotopes, Andover, MA). Q-band Mims three-pulse ENDOR spectra (*60*, *61*), pulse sequence, t_{mw}-tau-t_{mw}-T(rf)-t_{mw}-tau-echo, were obtained at 2 K on a locally designed spectrometer (*62*). The spectrum for a ^{13}C with a hyperfine coupling, A, is a doublet centered at the ^{13}C Larmor frequency and split by A. The intensity for a particular hyperfine coupling, A, is suppressed, creating a so-called 'Mims suppression hole', when A and tau satisfy the relation: $A\text{tau} = n$ (0, 1, 2, ...). The bandwidth of the radio frequency (RF) is broadened to 100 kHz to increase the signal-to-noise ratio (*63*). Spectra for a particular field within the EPR envelope of a frozen solution are associated with a well-defined subset of orientations, and simulations of a '2-D' set of such spectra can yield full hyperfine tensors, as discussed (*64*, *65*).

RESULTS

Acetylene Interactions. Substitution of the α-96^{Arg} residue by Ala, Leu, His, or Gln did not significantly change the line shape or intensity of the resting state $S = 3/2$ FeMo-cofactor EPR signal ($g = 4.26$, 3.67, 2.00) from that recorded for the wild-type MoFe protein (Figure 2 and Supporting Information). Minor EPR inflections were observed in some of the substituted MoFe proteins, but none of these constituted a significant species. The α-96^{Leu} MoFe protein was representative of the other α-96-substituted MoFe proteins. An earlier EPR investigation of the resting state of an α-96^{Gln} MoFe protein (*49*) revealed a similar spectrum. The lack of significant perturbations of the EPR signal for the α-96-substituted MoFe proteins suggests little or no changes in the electronic properties of FeMo-cofactor as a consequence

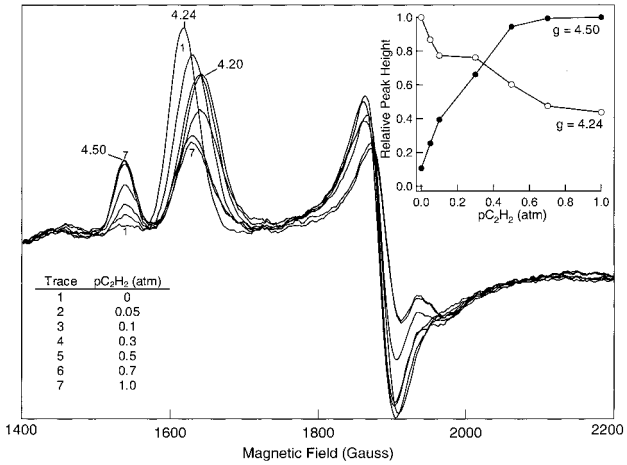

FIGURE 3: Effect of acetylene concentration on the EPR spectrum of α-96^{Leu} MoFe protein under nonturnover conditions. The α-96^{Leu} MoFe protein was incubated under a gas phase containing the indicated partial pressures of acetylene with argon added to a total pressure of 1 atm. The X-band EPR spectra were recorded at a temperature of 5 K, and a microwave power of 2.0 mW, and represent the sum of 5 scans. The inset shows the relationship between the EPR signal peak height for the $g = 4.24$ (○) and $g = 4.50$ (●) inflections versus the acetylene partial pressure (pC_2H_2).

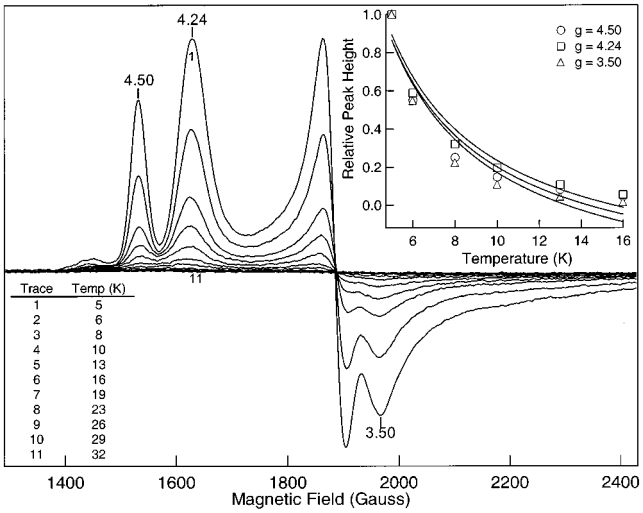

FIGURE 4: Temperature dependence of the EPR spectrum of the α-96^{Leu} MoFe protein under nonturnover conditions with acetylene. The α-96^{Leu} MoFe protein was prepared under a gas phase containing 1 atm of acetylene, and EPR spectra were acquired at the indicated temperatures with a microwave power of 0.32 mW. Each spectrum is the sum of 5 scans. The inset shows the relationship between EPR signal peak height for the $g = 4.50$ (○), 4.24 (□), and 3.50 (△) inflections as a function of temperature. The data are fit to Curie law $1/T$ dependence as described under Experimental Procedures.

of these substitutions. Earlier studies on the resting state of the wild-type MoFe protein found that changes in pH altered the $S = 3/2$ spin system of FeMo-cofactor (*66*, *67*). Addition of acetylene was found to perturb this pH effect, suggesting that acetylene could bind to the resting state of the MoFe protein. However, EPR (*28*, *66*) and EXAFS (*29*) studies found no evidence for direct binding of the acetylene or other substrates to FeMo-cofactor. In the present study, it is found that addition of acetylene to a resting state sample of the α-96^{Leu}-substituted MoFe protein results in the appearance of strong EPR inflections with g values at 4.50, 3.50, and <2.00 (Figure 2). Similar results were obtained with other α-96-substituted MoFe proteins, with slight differences in g values and line shape (Supporting Information). Changing the pH over the range from 6.5 to 8.5 for resting α-96^{Leu} MoFe protein did not mimic the acetylene-induced EPR inflections. Addition of the substrates dinitrogen or azide or the product ethylene also did not result in any detectable changes in the EPR spectrum (not shown). The acetylene-dependent changes in the EPR spectrum of the α-96^{Leu} MoFe protein were reversible as evidenced by a return to the original resting state EPR spectrum after removal of acetylene from the sample. The inclusion of CO or N_2 during incubation with acetylene did not prevent the appearance of the acetylene-dependent signal. Figure 3 shows the acetylene concentration dependence on the changes in the EPR spectrum. Increasing acetylene concentration results in a decrease in the intensity of the FeMo-cofactor signal (g values of 4.24 and 3.67 are shown) to a finite intensity approximately half the full intensity with a concomitant increase in the intensity of the new $g = 4.50$ inflection. The changes in the EPR spectrum saturate at 0.7 atm of acetylene, with half-saturation at approximately 0.2 atm of acetylene. This contrasts with a K_m for acetylene reduction during turnover of approximately 0.006 atm. It is noted that the $g = 4.24$ inflection arising from FeMo-cofactor changes g value with increasing acetylene partial pressure. Simulation of the α-96^{Leu} MoFe protein EPR spectrum at saturating acetylene concentration indicates that the acetylene-dependent signal constitutes approximately 40% of the total $S = 3/2$ EPR signal, with the remainder coming from the FeMo-cofactor signal detected in the absence of acetylene. Integration of the acetylene-dependent EPR signals combined with the remaining FeMo-cofactor signal represents >90% of the total spin determined for the FeMo-cofactor signal in the wild-type MoFe protein. These results suggest that acetylene addition to the α-96-substituted MoFe proteins result in the conversion of the FeMo-cofactor to a state exhibiting different electronic properties and different EPR g values. The temperature dependence of the EPR signal intensities is shown in Figure 4. The signal intensity of the FeMo-cofactor signal for the α-96^{Leu} MoFe protein ($g = 4.24$ is shown) decreases with increasing temperatures from 4 to 20 K, consistent with the behavior of the signal observed for FeMo-cofactor in wild-type MoFe protein. In both cases, the decrease in intensity closely follows Curie law $1/T$ dependence, indicating a ground-state transition. The acetylene-dependent EPR inflections observed in the α-96^{Leu} MoFe protein ($g = 4.50$ and 3.50 are shown) exhibit similar temperature dependence. This similarity indicates that the acetylene-dependent signal arises from a modified FeMo-cofactor species, maintaining the ground-state transition.

Cyanide Interactions. We also tested for CO and cyanide interaction with the resting state of the α-96^{Leu} MoFe protein. CO is not a substrate but is a powerful noncompetitive inhibitor of all nitrogenase substrates except protons (*13*). Analysis of the effect of cyanide is more complicated because it is both a nitrogenase substrate (HCN) and an inhibitor (CN^-) (*57*). Addition of CO to the resting state of the α-96^{Leu} MoFe protein resulted in no detectable changes in the EPR spectrum. In contrast, addition of cyanide to the α-96^{Leu} MoFe protein changed the EPR spectrum, with the appearance of a new inflection at $g = 4.06$ and minor inflections

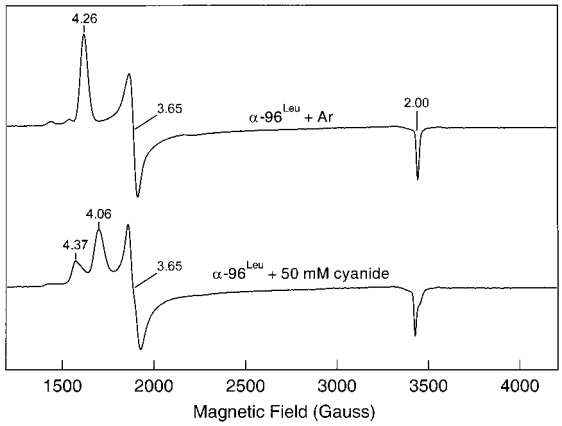

FIGURE 5: EPR spectra of α-96^{Leu} MoFe protein under nonturnover conditions with cyanide. The α-96^{Leu} MoFe protein was prepared under a gas phase of 1.0 atm of argon with no additions (top trace) or with the addition of 50 mM sodium cyanide (bottom trace). The X-band EPR spectra were recorded at a temperature of 5 K and a microwave power of 2.0 mW, and represent the sum of 5 scans.

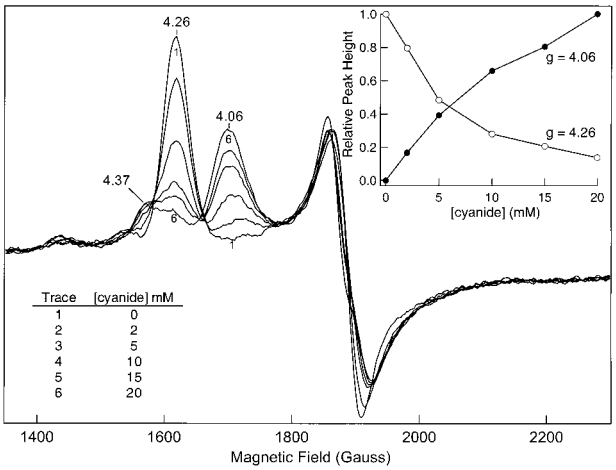

FIGURE 6: Effect of cyanide concentration on the EPR spectrum of α-96^{Leu} MoFe protein under nonturnover conditions. The α-96^{Leu} MoFe protein was prepared with the indicated sodium cyanide concentrations. The X-band EPR spectra were recorded at a temperature of 5 K and a microwave power of 2.0 mW, and represent the sum of 5 scans. The inset shows the relationship between the EPR signal peak height for the $g = 4.26$ (○) and $g = 4.06$ (●) inflections versus the cyanide concentration.

at $g = 4.37$ and $g < 2.00$ (Figure 5). This change in the EPR spectrum was reversed upon removal of cyanide from the sample. Increasing cyanide concentration resulted in a decrease in the FeMo-cofactor signal intensity ($g = 4.26$ and 3.65 shown) with a concomitant increase in the intensity of the cyanide-dependent $g = 4.06$ and 4.37 signals (Figure 6). The changes in EPR signal intensity were found to saturate between 20 and 50 mM cyanide concentration, so 50 mM cyanide was used for saturating conditions. Simulation of the α-96^{Leu} MoFe protein EPR spectrum for saturating cyanide concentration indicates that the cyanide-dependent inflections constitute >50% of the total $S = 3/2$ EPR signal present, with the remainder coming from the normal FeMo-cofactor signal. Integration of the cyanide-dependent EPR signals combined with the remaining FeMo-cofactor signal represents >90% of the total spin determined for the FeMo-cofactor signal in the wild-type MoFe protein. The correlation in the changes of these signal intensities upon addition of cyanide suggests conversion of FeMo-cofactor to a new

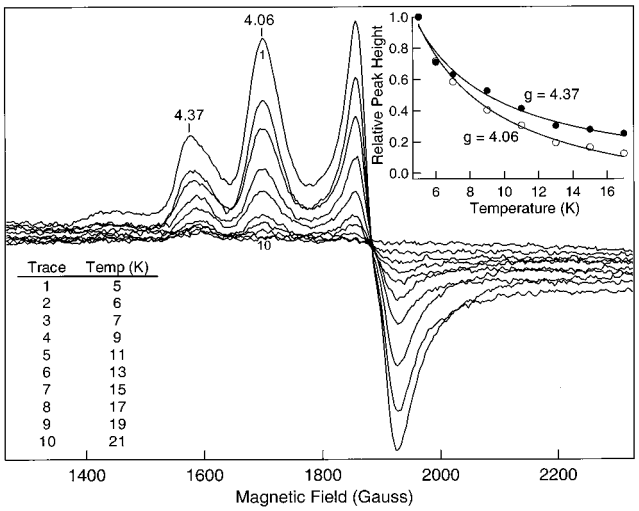

FIGURE 7: Temperature dependence of the EPR spectrum of the α-96^{Leu} MoFe protein when incubated in the presence of cyanide. The α-96^{Leu} MoFe protein was prepared with 50 mM sodium cyanide as described under Experimental Procedures. X-band EPR spectra were acquired at the indicated temperatures with a microwave power of 2.0 mW, and represent the sum of 5 scans. The inset shows the relationship between EPR signal peak height for the $g = 4.06$ (○) and 4.37 (●) signals as a function of temperature. The data are fit to the equation for Curie law $1/T$ dependence as described under Experimental Procedures.

species. The temperature dependence of the EPR signal intensities is shown in Figure 7. The cyanide-dependent EPR signal is observed to decrease in intensity upon increasing the temperature from 4 to 20 K, as is observed for FeMo-cofactor signals in wild-type MoFe protein. The temperature dependence follows Curie law $1/T$ dependence, suggesting a ground-state transition. No significant pH dependence was recognized for the EPR signal elicited by cyanide addition.

EPR Power Dependence. The microwave power dependence of EPR signals reflects the relaxation properties of the paramagnetic center. Figure 8 shows the Beinert−Orme−Johnson plot (*68*) of the dependence of the EPR signal intensities upon microwave power at 5 K for FeMo-cofactor signals from the α-96^{Leu} MoFe protein. The FeMo-cofactor EPR signals for wild-type (not shown) and α-96^{Leu} MoFe proteins saturate at approximately the same microwave power under these conditions, suggesting similar relaxation properties and a lack of perturbation by the amino acid substitution near FeMo-cofactor. The acetylene-dependent and cyanide-dependent EPR signals, in contrast, are observed to require slightly higher microwave power for saturation, indicating at least a partial inhibition of a relaxation process for these states.

^{13}C-ENDOR. The addition of cyanide to wild-type MoFe protein alone does not cause an observable change in its EPR spectrum (*29*), but [^{13}C]cyanide-incubated wild-type protein does exhibit a minor unresolved ENDOR signal at the ^{13}C Larmor frequency that is not present for MoFe protein treated with natural-abundance cyanide (Figure 9). The latter observation suggests a weak, nonspecific interaction of cyanide with FeMo-cofactor in the resting state MoFe protein. No ENDOR response was observed when the wild-type MoFe protein was treated with [^{13}C]acetylene.

The appearance of new EPR signals upon the addition of cyanide or acetylene to the α-96^{Leu}-substituted MoFe protein could result from conformational changes caused by interac-

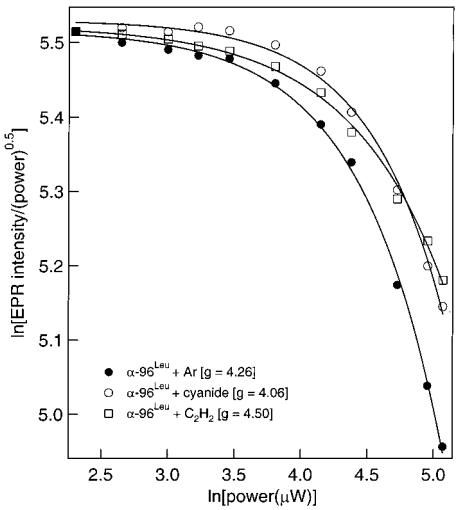

FIGURE 8: Microwave power dependencies of the EPR signals for the wild-type and α-96^{Leu} MoFe proteins. EPR signal intensities were determined for the $g = 4.26$ inflection of the α-96^{Leu} MoFe protein (●), the $g = 4.06$ inflection of the α-96^{Leu} MoFe protein with 50 mM cyanide (○), and the $g = 4.50$ inflection of the α-96^{Leu} MoFe protein under 1.0 atm of acetylene (□) at a constant temperature of 5 K, and at various microwave powers ranging from 0.1 to 25.3 mW. The natural logarithm of the normalized signal intensities divided by the square root of the microwave power is plotted against the natural logarithm of the microwave power. The data are fit to a single exponential.

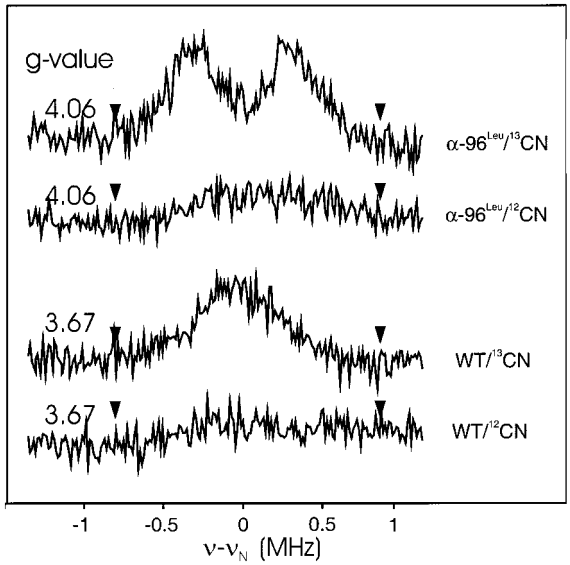

FIGURE 9: Q-band Mims ^{13}C-pulsed-ENDOR spectra of MoFe proteins with cyanide. The α-96^{Leu} MoFe or wild-type (WT) MoFe proteins were incubated with Na^{12}CN or Na^{13}CN as detailed under Experimental Procedures. The pulsed ENDOR conditions were: $T = 2$ K; microwave frequency, $\nu_{MW} = 34.86$ GHz; MW pulse lengths tmw = 52 ns, $\tau = 600$ ns, RF pulse length = 60 μs, and repetition rate = 20 Hz. Each spectrum consists of 256 points, with each point an average of 6000 transients for α-96^{Leu} MoFe protein samples and of 1000 transients for wild-type MoFe protein samples. The arrows point to the Mim's 'suppression holes'.

tions with distant locations, or from direct binding to the FeMo-cofactor. In an attempt to distinguish between these possibilities, the nature of the interaction of [^{13}C]cyanide- and [^{13}C]acetylene-treated samples was tested with pulsed ENDOR spectroscopy. We were unable to detect an ENDOR response with [^{13}C]-acetylene. However, it is not possible to draw any firm conclusion from this negative result because

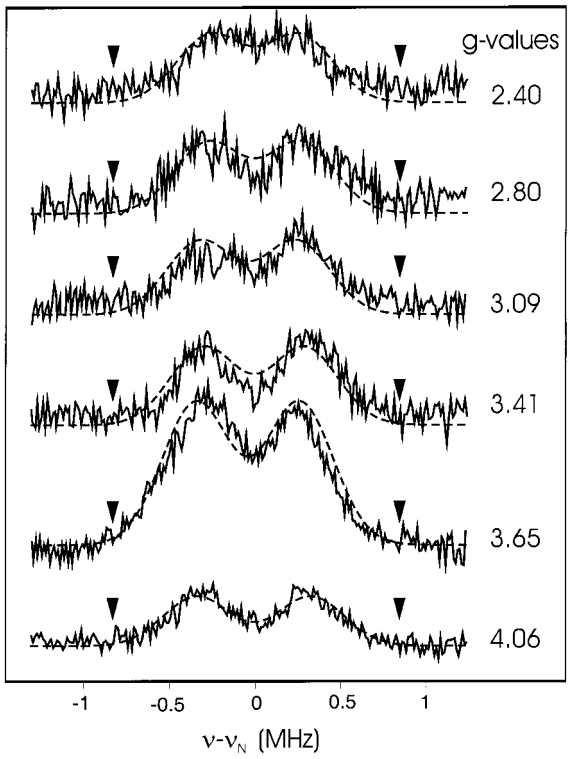

FIGURE 10: Q-band Mims ^{13}C-pulsed-ENDOR spectra of α-96^{Leu} MoFe protein with ^{13}C-labeled cyanide across the entire EPR envelope. The pulsed ENDOR conditions were the same as in Figure 9. Theoretical simulations (dashed lines) were done as described under Experimental Procedures. The arrows point to the Mim's holes.

we were not able to consistently prepare samples with protein concentrations much greater than 100 mg/mL. In contrast, a clear ENDOR response was observed upon addition of [^{13}C]-cyanide to the α-96^{Leu}-substituted MoFe protein. Figure 9 shows a well-resolved ^{13}C doublet centered at the ^{13}C Larmor frequency that is not observed with natural-abundance cyanide. Figure 10 shows the 2D plot of ^{13}C ENDOR spectra taken across the EPR envelope (from $g = 2.40$ to 4.06) of [^{13}C]cyanide-incubated α-96^{Leu} MoFe protein (solid line). The spectra include simulations based on an axial ^{13}C hyperfine coupling tensor in the true-spin, $S = 3/2$ representation, that is coaxial with the **g**-tensor frame; it can be decomposed into an isotropic coupling of $a_{iso} = 0.42$ MHz and an axial traceless part with a coupling parameter of $T = 0.07$ MHz.

DISCUSSION

The results presented here show that the α-96^{Leu}-, α-96^{His}, α-96^{Ala}, and α-96^{Gln}-substituted MoFe proteins are able to bind acetylene or cyanide in the resting state. Simulations of the cyanide- and acetylene-induced EPR signals indicate that they arise from the $S = 3/2$ system of FeMo-cofactor. Furthermore, the temperature dependence of the intensities for the cyanide- and acetylene-induced signals is similar to that observed for FeMo-cofactor. All of the signals follow Curie law $1/T$ dependence, suggesting that they are from ground-state transitions. This feature is important because several oxidation states of the P-cluster are EPR-active, with each state exhibiting excited-state temperature dependence (*69*−*71*). Thus, the observation of a ground-state transition for the cyanide- and acetylene-dependent EPR signals

indicates they arise from FeMo-cofactor rather than from the P-clusters. The shift to higher microwave power saturation for the cyanide- and acetylene-dependent EPR signals is indicative of some inhibition of a relaxation event (*68*), which is consistent with the binding of cyanide or acetylene.

Changes in the EPR signals for α-96-substituted MoFe proteins elicited by addition of cyanide or acetylene can be explained in two different ways. One possibility is that acetylene or cyanide binds to the protein near, but not directly to, the FeMo-cofactor, and thereby changes the electronic properties of the FeMo-cofactor indirectly. Alternatively, acetylene or cyanide could bind directly to the FeMo-cofactor. Although we were unable to resolve this question with respect to acetylene binding, ^{13}C ENDOR spectroscopy was used to distinguish between these possibilities in the case of cyanide binding. The observation of a ^{13}C doublet for the [^{13}C]cyanide-treated α-96^{Leu} MoFe protein with a derived isotropic coupling of 0.42 MHz supports the existence of some electron spin density on the cyanide, which in turn requires that cyanide bind directly to the FeMo-cofactor. The coupling constant of 0.42 MHz is comparable to ^{13}C hyperfine couplings (0.5−5 MHz) observed from ^{13}CO (*33*, *34*), $^{13}CS_2$ (*40*), and [^{13}C]acetylene (*38*) binding to FeMo-cofactor in MoFe protein trapped during catalytic turnover. These values are very different from the coupling constants observed for ^{13}CO or [^{13}C]cyanide bound to the active sites of other metalloenzymes (e.g., >20 MHz). From ^{13}C ENDOR studies with ^{13}CO and isotopically labeled MoFe protein, it was concluded that CO binds to one or more Fe atoms in FeMo-cofactor (*33*). The similar ^{13}C-ENDOR hyperfine coupling observed here for [^{13}C]cyanide binding to the α-96^{Leu} MoFe protein strongly suggests that cyanide is binding to one or more Fe atom(s) of FeMo-cofactor as well. Additional evidence that cyanide is bound directly to FeMo-cofactor when added to the resting state of the α-96^{Leu} MoFe protein is that the new EPR spectrum is strikingly similar to that recognized when cyanide is added to the isolated FeMo-cofactor (*72*). From those studies with isolated FeMo-cofactor, it was suggested that cyanide had at least two binding sites. The results presented in the present work do not specifically address the number of cyanide molecules bound, but could be explained by the binding of just one cyanide. The possible differences in cyanide binding to FeMo-cofactor extracted into organic solvent compared to FeMo-cofactor bound within the MoFe protein could be accounted for by the protein environment blocking a cyanide binding site.

α-*96^{Arg} as Gatekeeper*. Our original reason for testing if substrates or inhibitors can interact with α-96-substituted MoFe proteins in the resting state was based on analysis of an altered protein having α-69^{Ser} substituted at the α-69^{Gly} position. This substitution results in an altered MoFe protein having a dramatically increased K_m for acetylene reduction with very little or no effect on proton or dinitrogen reduction (*42*, *43*). From those studies, we proposed that the [4Fe-4S] face of FeMo-cofactor that is capped by α-70^{Val} provides a site for acetylene interaction (Figure 1, panels A and B). Inspection of the crystal structure of the resting state MoFe protein shows that all three [4Fe-4S] faces of FeMo-cofactor are so tightly packed with amino acid side chains there appears to be no room to accommodate substrate interaction. Thus, if substrates do interact with the [4Fe-4S] face approached by α-70^{Val} and α-96^{Arg}, then either or both of their side chains would have to move under turnover to permit substrate interaction. The addition of acetylene or cyanide to the wild-type or α-70^{Ala}-substituted MoFe proteins has no effect on the resting state $S = 3/2$ EPR spectrum. In contrast, as shown here, altered MoFe proteins having α-96^{Arg} substituted with leucine, glutamine, alanine, or histidine are able to interact with acetylene or cyanide. In contrast, substitution of α-96^{Arg} with lysine does not allow changes in the EPR spectrum when acetylene or cyanide is added. The longer side chain of lysine would be expected to act like arginine, blocking access to FeMo-cofactor. These results are consistent with a model where the α-96^{Arg} side chain in the wild-type protein acts as a gatekeeper, repositioning during turnover to expose a substrate or inhibitor interaction site.

While the results presented here are consistent with α-96^{Arg} functioning as a gatekeeper, it seems unlikely for two reasons that this side chain is the only feature involved in controlling substrate or inhibitor interaction with FeMo-cofactor. First, the concentration of cyanide or acetylene necessary to elicit a significant perturbation in the $S = 3/2$ EPR spectrum for the altered proteins in the resting state is much greater than required for detecting substrate reduction under turnover conditions. This situation could be an indication that repositioning of other amino acid side chains, in addition to α-96^{Arg}, also occurs during turnover to facilitate effective substrate interaction. Such protein conformational changes could open channels for substrate movement from the protein surface to FeMo-cofactor (*73*). Second, the addition of dinitrogen, azide, CO, or ethylene to samples of α-96-substituted MoFe protein has no effect on the resting state $S = 3/2$ EPR spectra of the variously substituted MoFe proteins. It is difficult to imagine that, based only on steric considerations, substitutions at this position would permit FeMo-cofactor interaction with acetylene or cyanide but not with CO, azide, or dinitrogen. A reasonable explanation is that both the reactivity and accessibility of FeMo-cofactor toward substrates and inhibitors increase as the MoFe protein becomes more reduced. Thus, although dinitrogen, azide, and CO could have access to the active site of α-96-substituted MoFe proteins, FeMo-cofactor might not be sufficiently reactive in the resting state to permit detectable interaction. This explanation is consistent with suggestions from model compound studies that reduction could change bonding interactions to or within FeMo-cofactor, rendering Fe atoms more reactive (*74*). This idea is particularly attractive in the case of dinitrogen binding because extensive kinetic analyses have shown that its binding to the MoFe protein requires a more reduced state of the enzyme than does either acetylene or cyanide (*43*, *57*, *75*, *76*). This possibility is also supported by the observation that cyanide interaction can be detected with isolated FeMo-cofactor (*29*, *72*, *77*) in the dithionite-reduced state.

It is possible that acetylene and cyanide interaction detected for the α-96-substituted MoFe proteins is not relevant to catalysis but instead reflects the opening of a fortuitous binding site. We do not favor this interpretation because the α-70^{Ala}-substituted MoFe protein is able to effectively reduce propyne, indicating that substrates are able to bind *and be reduced* near the [4Fe-4S] face of FeMo-cofactor approached by this residue (*44*). Also, the α-96^{Leu}-

substituted MoFe protein has a significant change in proton addition stereospecificity for acetylene reduction, as well as a decreased K_m for acetylene reduction (*56*), supporting the view that acetylene binding and reduction also occur at this same [4Fe-4S] face.

It is noteworthy that the [4Fe-4S] face of FeMo-cofactor that is capped by α-70 and α-96 is in the best position for communication with the P-cluster. This face is the closest of the three [4Fe-4S] faces to the P-cluster, which is believed to be the intermediate site for electron delivery to the FeMo-cofactor. Moreover, both $\alpha\text{-}70^{Val}$ and $\alpha\text{-}96^{Arg}$ are ideally positioned for sensing conformational changes in the P-cluster because they are connected through short helices to the P-cluster ligands $\alpha\text{-}62^{Cys}$ and $\alpha\text{-}88^{Cys}$, respectively (Figure 1C). Also, because the P-cluster itself is known to undergo redox-dependent rearrangement (*6*), it is possible that such changes are communicated to the FeMo-cofactor through movement of either or both $\alpha\text{-}70^{Val}$ and $\alpha\text{-}96^{Arg}$.

In conclusion, demonstration that cyanide and acetylene can bind to the resting state of the α-96-substituted MoFe protein now provides an opportunity to study ligand binding to FeMo-cofactor contained within the MoFe protein. In particular, solving the X-ray structure of the MoFe protein with cyanide or acetylene bound would provide insight into how substrates interact with the nitrogenase active site.

ACKNOWLEDGMENT

We thank Drs. Jeannine Chan and Jennifer Huyett for technical assistance, Dr. Mike Hendrich of Carnegie Mellon University for EPR simulations (hendrich@andrew.cmu.edu), Dr. Brain Bennett of the Medical College of Wisconsin (bbennett@mcw.edu) for discussions on EPR, and Valerie Cash for strain constructions.

SUPPORTING INFORMATION AVAILABLE

Supporting information is available showing the EPR spectra for the $\alpha\text{-}96^{His}$, $\alpha\text{-}96^{Gln}$, and $\alpha\text{-}96^{Ala}$ MoFe proteins with or without acetylene or cyanide (1 page). This material is available free of charge via the Internet at http://pubs.acs.org.

REFERENCES

1. Rees, D. C., and Howard, J. B. (2000) *Curr. Opin. Chem. Biol. 4*, 559−566.
2. Burgess, B. K., and Lowe, D. J. (1996) *Chem. Rev. 96*, 2983−3011.
3. Christiansen, J., Chan, J. M., Seefeldt, L. C., and Dean, D. R. (2000) in *Prokaryotic Nitrogen Fixation: A Model System for Analysis of a Biological Process* (Triplett, E., Ed.) pp 101−112, Horizon Scientific Press, Wymondham, U.K.
4. Georgiadis, M. M., Komiya, H., Chakrabarti, P., Woo, D., Kornuc, J. J., and Rees, D. C. (1992) *Science 257*, 1653−1659.
5. Seefeldt, L. C., and Dean, D. R. (1997) *Acc. Chem. Res. 30*, 260−266.
6. Peters, J. W., Stowell, M. H. B., Soltis, S. M., Finnegan, M. G., Johnson, M. K., and Rees, D. C. (1997) *Biochemistry 36*, 1181−1187.
7. Bolin, J. T., Ronco, A. E., Mortenson, L. E., Morgan, T. V., Williamson, M., and Xuong, N. H. (1990) in *Nitrogen Fixation: Achievements and Objectives* (Gresshoff, P. M., Roth, L. E., Stacey, G., and Newton, W. E., Eds.) pp 117−122, Chapman and Hall, New York.
8. Kim, J., and Rees, D. C. (1992) *Nature 360*, 553−560.
9. Nyborg, A. C., Johnson, J. L., Gunn, A., and Watt, G. D. (2000) *J. Biol. Chem. 275*, 39307−39312.
10. Burgess, B. K. (1990) *Chem. Rev. 90*, 1377−1406.
11. Hageman, R. V., and Burris, R. H. (1978) *Proc. Natl. Acad. Sci. U.S.A. 75*, 2699−2702.
12. Thorneley, R. N. F., and Lowe, D. J. (1985) in *Molybdenum Enzymes* (Spiro, T. G., Ed.) pp 221−284, Wiley, New York.
13. Burgess, B. K. (1985) in *Metal Ions in Biology: Molybdenum Enzymes* (Spiro, T. G., Ed.) pp 161−220, John Wiley and Sons, New York.
14. Chan, M. K., Kim, J., and Rees, D. C. (1993) *Science 260*, 792−794.
15. Kim, J., and Rees, D. C. (1992) *Science 257*, 1677−1682.
16. Kim, J., Woo, D., and Rees, D. C. (1993) *Biochemistry 32*, 7104−7115.
17. Mayer, S. M., Lawson, D. M., Gormal, C. A., Roe, S. M., and Smith, B. E. (1999) *J. Mol. Biol. 292*, 871−891.
18. Dance, I. G. (1994) *Aust. J. Chem. 47*, 979−990.
19. Sellmann, D. (1999) *Coord. Chem. Rev. 190*, 607−627.
20. Deng, H., and Hoffmann, R. (1993) *Angew. Chem., Int. Ed. Engl. 32*, 1062−1065.
21. Dance, I. (1998) *Chem. Commun.*, 523−530.
22. Sellmann, D., Fursattel, A., and Sutter, J. (2000) *Coord. Chem. Rev. 200−202*, 545−561.
23. Siegbahn, P. E. M., and Blomberg, M. R. A. (1999) *Annu. Rev. Phys. Chem. 50*, 221−249.
24. Stavrev, K. K., and Zerner, M. C. (1998) *Int. J. Quantum Chem. 70*, 1159−1168.
25. Pickett, C. J. (1996) *J. Biol. Inorg. Chem. 1*, 601−606.
26. Lehnert, N., Wiesler, B. E., Tuczek, F., Hennige, A., and Sellmann, D. (1997) *J. Am. Chem. Soc. 119*, 8869−8878.
27. Rod, T. H., and Norskov, J. K. (2000) *J. Am. Chem. Soc. 122*, 12751−12763.
28. Howes, B. D., Fisher, K., and Lowe, D. J. (1994) *Biochem. J. 297*, 261−264.
29. Conradson, S. D., Burgess, B. K., Vaughn, S. A., Roe, A. L., Hedman, B., Hodgson, K. O., and Holm, R. H. (1989) *J. Biol. Chem. 264*, 15967−15974.
30. Yates, M. G., and Lowe, D. J. (1976) *FEBS Lett. 72*, 121−126.
31. Davis, L. C., Henzl, M. T., Burris, R. H., and Orme-Johnson, W. H. (1979) *Biochemistry 18*, 4860−4869.
32. Pollock, C. R., Lee, H.-I., Cameron, L. M., DeRose, V. J., Hales, B. J., Orme-Johnson, W. H., and Hoffman, B. M. (1995) *J. Am. Chem. Soc. 117*, 8686−8687.
33. Christie, P. D., Lee, H. I., Cameron, L. M., Hales, B. J., Orme-Johnson, W. H., and Hoffman, B. M. (1996) *J. Am. Chem. Soc. 118*, 8707−8709.
34. Lee, H. I., Cameron, L. M., Hales, B. J., and Hoffman, B. M. (1997) *J. Am. Chem. Soc. 119*, 10121−10126.
35. George, S. J., Ashby, G. A., Wharton, C. W., and Thorneley, R. N. F. (1997) *J. Am. Chem. Soc. 119*, 6450−6451.
36. Lowe, D. J., Fisher, K., and Thorneley, R. N. F. (1993) *Biochem. J. 292*, 93−98.
37. Lowe, D. J., Eady, R. R., and Thorneley, R. N. F. (1978) *Biochem. J. 173*, 277−290.
38. Lee, H. I., Sorlie, M., Christiansen, J., Song, R., Dean, D. R., Hales, B. J., and Hoffman, B. M. (2000) *J. Am. Chem. Soc. 122*, 5582−5587.
39. Fisher, K., Newton, W. E., and Lowe, D. J. (2001) *Biochemistry 40*, 3333−3339.
40. Ryle, M. J., Lee, H. I., Seefeldt, L. C., and Hoffman, B. M. (2000) *Biochemistry 39*, 1114−1119.
41. Hawkes, T. R., Lowe, D. J., and Smith, B. E. (1983) *Biochem. J. 211*, 495−497.
42. Christiansen, J., Cash, V. L., Seefeldt, L. C., and Dean, D. R. (2000) *J. Biol. Chem. 275*, 11459−11464.
43. Christiansen, J., Seefeldt, L. C., and Dean, D. R. (2000) *J. Biol. Chem. 275*, 36104−36107.
44. Mayer, S. M., Niehaus, W. G., and Dean, D. R. (2001) *Dalton Trans.* (in press).
45. Dilworth, M. J., Fisher, K., Kim, C. H., and Newton, W. E. (1998) *Biochemistry 37*, 17495−17505.

46. Fisher, K., Dilworth, M. J., Kim, C. H., and Newton, W. E. (2000) *Biochemistry 39*, 2970−2979.
47. Fisher, K., Dilworth, M. J., Kim, C. H., and Newton, W. E. (2000) *Biochemistry 39*, 10855−10865.
48. Fisher, K., Dilworth, M. J., and Newton, W. E. (2000) *Biochemistry 39*, 15570−15577.
49. Lee, H. I., Thrasher, K. S., Dean, D. R., Newton, W. E., and Hoffman, B. M. (1998) *Biochemistry 37*, 13370−13378.
50. DeRose, V. J., Kim, C. H., Newton, W. E., Dean, D. R., and Hoffman, B. M. (1995) *Biochemistry 34*, 2809−2814.
51. Kim, C. H., Newton, W. E., and Dean, D. R. (1995) *Biochemistry 34*, 2798−2808.
52. Scott, D. J., May, H. D., Newton, W. E., Brigle, K. E., and Dean, D. R. (1990) *Nature 343*, 188−190.
53. Seefeldt, L. C., Morgan, T. V., Dean, D. R., and Mortenson, L. E. (1992) *J. Biol. Chem. 267*, 6680−6688.
54. Burgess, B. K., Jacobs, D. B., and Stiefel, E. I. (1980) *Biochim. Biophys. Acta 614*, 196−209.
55. Christiansen, J., Goodwin, P. J., Lanzilotta, W. N., Seefeldt, L. C., and Dean, D. R. (1998) *Biochemistry 37*, 12611−12623.
56. Benton, P. M. C., Christiansen, J., Dean, D. R., and Seefeldt, L. C. (2001) *J. Am. Chem. Soc. 123*, 1822−1827.
57. Li, J., Burgess, B. K., and Corbin, J. L. (1982) *Biochemistry 21*, 4393−4402.
58. Feher, G. (1959) *Phys. Rev. 114*, 1219−1244.
59. Mailer, C., and Taylor, C. P. (1973) *Biochim. Biophys. Acta 322*, 195−203.
60. Schweiger, A. (1991) *Angew. Chem., Int. Ed. Engl. 30*, 265−292.
61. Grupp, A., and Mehring, M. (1990) in *Modern Pulsed and Continuous-Wave Electron Spin Resonance* (Kevan, L., and Bowman, M. K., Eds.) pp 195−229, Wiley and Sons, New York.
62. Hoffman, B. M., DeRose, V. J., Ong, J.-L., and Davoust, C. E. (1994) *J. Magn. Reson., Ser. A 110*, 52−57.
63. Davoust, C. E., Doan, P. E., and Hoffman, B. M. (1996) *J. Magn. Reson. 119*, 38−44.
64. Hoffman, B. M., DeRose, V. J., Doan, P. E., Gurbiel, R. J., Houseman, A. L. P., and Telser, J. (1993) in *Biological Magnetic Resononance* (Berliner, L. J., and Reuben, J., Eds.) pp 151−218, Plenum Press, New York.
65. DeRose, V. J., and Hoffman, B. M. (1995) in *Methods in Enzymology* (Sauer, K., Ed.) pp 555−589, Academic Press, New York.
66. Smith, B. E., Lowe, D. J., and Bray, R. C. (1973) *Biochem. J. 135*, 331−341.
67. Smith, B. E. (1983) in *Nitrogen Fixation: The Chemical-Biochemical-Genetic Interface* (Muller, A., and Newton, W. E., Eds.) pp 23−63, Plenum Press, New York.
68. Beinert, H., and Orme-Johnson, W. H. (1967) in *Magnetic Resonance in Biological Systems* (Ehrenberg, A., Malmstrom, B. G., and Vanngard, T., Eds.) pp 221−247, Pergamon Press, New York.
69. Tittsworth, R. C., and Hales, B. J. (1993) *J. Am. Chem. Soc. 115*, 9763−9767.
70. Pierik, A. J., Wassink, H., Haaker, H., and Hagen, W. R. (1993) *Eur. J. Biochem. 212*, 51−61.
71. Hagen, W. R., Wassink, H., Eady, R. R., Smith, B. E., and Haaker, H. (1987) *Eur. J. Biochem. 169*, 457−465.
72. Richards, A. J. M., Lowe, D. J., Richards, R. L., Thomson, A. J., and Smith, B. E. (1994) *Biochem. J. 297*, 373−378.
73. Durrant, M. C. (2001) *Biochem. J. 355*, 569−576.
74. Han, J., Beck, K., Ockwig, N., and Coucouvanis, D. (1999) *J. Am. Chem. Soc. 121*, 10448−10449.
75. Lowe, D. J., Fisher, K., and Thorneley, R. N. F. (1990) *Biochem. J. 272*, 621−625.
76. Shen, J., Dean, D. R., and Newton, W. E. (1997) *Biochemistry 36*, 4884−94.
77. Liu, H. I., Filipponi, A., Gavini, N., Burgess, B. K., Hedman, B., Di Cicco, A., Natoli, C. R., and Hodgson, K. O. (1994) *J. Am. Chem. Soc. 116*, 2418−2423.
78. Geux, N., and Peitsch, M. C. (1997) *Electrophoresis 18*, 2714−2723.

BI011571M